RAPID COMMUNICATIONS

PHYSICAL REVIEW E VOLUME 48, NUMBER 1 JULY 1993

Scaling of structure functions

G. Stolovitzky and K. R. Sreenivasan
Mason Laboratory, Yale University, New Haven, Connecticut 06520-2159
(Received 8 March 1993)

In a recent paper, Benzi *et al.* [Università di Roma, Report No. ROM 2F/92/54 (unpublished)] proposed that an extensive scaling region can be observed—even at moderate Reynolds numbers—when the structure functions of arbitrary order are plotted against the third-order structure function, and that the scaling region in such plots encompasses both inertial and dissipative ranges. This notion of extended self-similarity is analyzed here, and it is found that the concept is valid when it entails low-order structure functions, but that the scaling in the inertial and dissipation regions differs clearly for high orders. The same is true also for moments of the absolute value of velocity increments.

PACS number(s): 05.45.+b, 02.50.−r, 03.40.Gc, 47.27.−i

Much work has been devoted in the last few decades to the measurement and modeling of the scaling of structure functions in turbulent flows. The structure function of order n is defined as $\langle \Delta u(r)^n \rangle$, where $\Delta u(r) = u(\mathbf{x}+\mathbf{r}) - u(\mathbf{x})$ and $u(\mathbf{x})$ is the velocity component at the position $\mathbf{x}$ parallel to the relative displacement, $r = |\mathbf{r}|$. For r in the inertial range of scales, $\eta \ll r \ll L$ (where η is the Kolmogorov scale and L is the outer scale), the expectation [1,2] is that $\langle \Delta u(r)^n \rangle \sim r^{\zeta_n}$. This scaling of the structure functions is an indication of scale invariance in turbulence.

In practice, the inertial range is usually defined as the r region in which Kolmogorov's $\frac{4}{5}$ law [3] holds, namely,

$$\langle \Delta u(r)^3 \rangle = -\tfrac{4}{5} \langle \varepsilon \rangle r \ , \tag{1}$$

where $\langle \varepsilon \rangle$ is the average energy dissipation rate per unit mass ε. The larger the Reynolds number, the larger is this range. For the low-to-moderate Reynolds-number turbulence with which one often deals, the inertial scaling range is uncomfortably small.

In a recent paper [4], Benzi *et al.* made an intriguing proposal for extending the region of observed scale similarity. Instead of plotting the logarithm of the structure functions against $\log_{10}(r)$, they plotted them against the logarithm of the modulus of the third-order structure function. Since the latter should scale as r [Eq. (1)] in the inertial range, it follows that such a plot should be similar to plots of $\log_{10}|\langle \Delta u(r)^n \rangle|$ versus $\log_{10}(r)$. According to Benzi *et al.*, the advantage of their proposal is that the scaling region extends to the dissipative range, so that the inertial-range relations

$$|\langle \Delta u(r)^n \rangle| = M_n |\langle \Delta u(r)^3 \rangle|^{\zeta_n} \tag{2a}$$

hold almost all the way to η. Here M_n are constants independent of r. In Ref. [4], it was stated that this is true also for moments of the absolute value of velocity increments. The equivalent relations in this case are

$$\langle |\Delta u(r)|^n \rangle = N_n \langle |\Delta u(r)^3| \rangle^{\zeta_n^*} \ , \tag{2b}$$

where the constants N_n are independent of r. For brevity, the two schemes (2a) and (2b) will be referred to, respectively, as case C (classical case) and case A (the case with absolute values). The relation between the exponents in Eqs. (2a) and (2b) is not known *a priori*. Although it is quite often implied that they are the same (e.g., Ref. [4]), it will be shown here that they differ at least in one respect.

A precedent to Eq. (2a) was put forward by Obukhov in 1949 (Ref. [1], p. 403). Assuming the skewness of the longitudinal velocity increment $S(r) = \langle \Delta u(r)^3 \rangle / \langle \Delta u(r)^2 \rangle^{3/2}$ to be a (negative) constant independent of r, Obukhov rewrote the Kolmogorov equation for the third-order structure function [3] as a closed equation for the second-order structure function. This closure scheme, however, has the drawback of yielding a negative-energy spectrum for a part of the wave-number range. Equation (2) with $n=2$ can be considered a refinement of Obukhov's assumption, where the exponent ζ_2 incorporating small-scale intermittency replaces the classical Kolmogorov value [5] of $\frac{2}{3}$. Further, Eqs. (2a) and (2b) extend the assumption to all $n \geq 2$, and hence are more ambitious.

Benzi *et al.* showed evidence for this so-called extended self-similarity by plotting $\langle |\Delta u(r)^n| \rangle$ versus $\langle |\Delta u(r)^3| \rangle$ for $n=2$. They stated that similar plots for higher n would allow unambiguous evaluation of the exponents ζ_n^*, and presented data up to order 8. They further stated that the same results would hold if $|\langle \Delta u(r)^n \rangle|$ were plotted against $|\langle \Delta u(r)^3 \rangle|$.

Since the notion of extended self-similarity, if true, is potentially important, we have repeated the measurements of Benzi *et al.* using velocity data at a moderate Reynolds number in a turbulent boundary layer on a flat plate. We had previously [6] obtained very long data records (10^7 sample points), which allowed us to obtain converged moments of high order (at least up to the order 15) [7]. The analysis of these data reveals that, for low-order moments, a single fit suffices (within statistical uncertainties) for dissipative as well as inertial ranges. However, as the order of the moment increases, the inertial and dissipation regions separate out, and the extended self-similarity does not hold. For case C, the scaling

exponents within the dissipative range are given by $n/3$, at least up to the order of the moment considered here; Benzi *et al.* termed them as "naive" values in the sense that they are to be expected for $r \sim \eta$. Further, the exponents in the inertial range are nonmonotonic with odd- and even-order values falling on separate curves. Thus a plot of $\log_{10}|\langle \Delta u(r)^n \rangle|$ versus $\log_{10}|\langle \Delta u(r)^3 \rangle|$ consists of one linear region of slope $n/3$ for small r and another linear region of slope ζ_n for r in the inertial range, joined by a smooth transitional region. The ζ_n's for small values of n (say, $n<4$) are not far from $n/3$, and so the structure-function plots appear to have a single straight line; however, the differences between the two regimes become increasingly apparent for higher n. The situation is similar for the case A: plots of $\log_{10}\langle |\Delta u(r)^n| \rangle$ versus $\log_{10}\langle |\Delta u(r)^3| \rangle$ have slopes of $(n/2+\zeta_{3n/2})/(3/2+\zeta_{9/2})$ in the dissipation range, and smoothly merge with the inertial scaling, Eq. (2b). Again, the differences between the two slopes are clear when high-order moments are considered. In spite of this partially negative conclusion about the extended self-similarity, this novel way of plotting structure functions possesses some interesting new features, which we shall explore below.

Dissipative range, case C: A Taylor expansion to first order in r yields $\langle \Delta u(r)^n \rangle = \langle (du/dx)^n \rangle r^n$, and we trivially have

$$\log_{10}|\langle \Delta u(r)^n \rangle| = \log_{10}|\langle (du/dx)^n \rangle| + n \log_{10}(r) \ . \tag{3}$$

By solving Eq. (3) with $n=3$ for $\log_{10}(r)$ and substituting $\log_{10}(r)$ back into Eq. (3), it is immediately seen that

$$\log_{10}|\langle \Delta u(r)^n \rangle| = \log_{10}|\langle (du/dx)^n \rangle| - \frac{n}{3}\log_{10}|\langle (du/dx)^3 \rangle| + \frac{n}{3}\log_{10}|\langle \Delta u(r)^3 \rangle| \ . \tag{4}$$

It can be expected that Eq. (4) will be valid in the range of $r \sim \eta$.

To determine the scaling for a more extensive range of r values, we expand $\Delta u(r)$ to third order in r:

$$\langle \Delta u(r)^n \rangle = \left\langle \left[\frac{du}{dx} r + \frac{d^2u}{dx^2}\frac{r^2}{2} + \frac{d^3u}{dx^3}\frac{r^3}{6} + \cdots \right]^n \right\rangle \ . \tag{5}$$

Expanding the right-hand side of Eq. (5) and systematically retaining terms to order r^{n+2}, we obtain

$$\langle \Delta u(r)^n \rangle = A_n r^n + B_n r^{n+1} + C_n r^{n+2} \ , \tag{6}$$

where

$$A_n = \left\langle \left[\frac{du}{dx} \right]^n \right\rangle , \quad B_n = \frac{n}{2}\left\langle \frac{d^2u}{dx^2}\left[\frac{du}{dx} \right]^{n-1} \right\rangle \tag{7}$$

and

$$C_n = \frac{n}{6}\left\langle \frac{d^3u}{dx^3}\left[\frac{du}{dx} \right]^{n-1} \right\rangle + \frac{n(n-1)}{8}\left\langle \left[\frac{d^2u}{dx^2} \right]^2 \left[\frac{du}{dx} \right]^{n-2} \right\rangle \ . \tag{8}$$

It can be easily shown that $B_n = 0$, and that Eq. (8) can be reduced to

$$C_n = \frac{n}{24}\left\langle \frac{d^3u}{dx^3}\left[\frac{du}{dx} \right]^{n-1} \right\rangle \ . \tag{9}$$

In the dissipation region, it is reasonable to take $d/dx = O(\eta^{-1})$, so that

$$\frac{d^3u}{dx^3} = \frac{K'(x)}{\eta^2}\frac{du}{dx} \ . \tag{10}$$

The proportionality factor $K'(x)$ can be either positive or negative, and its magnitude is of order of unity. Equation (9) then becomes

$$|C_n| = (K/\eta^2)\frac{n}{24}\left| \left\langle \left[\frac{du}{dx} \right]^n \right\rangle \right| = (K/\eta^2)\frac{n}{24}|A_n| \ , \tag{11}$$

where the constant K incorporates the integrated effect on K', and is smaller than K'. For $n=2$ it can be rigorously shown that $K = S/\sqrt{60} \sim 0.06$, where S is the velocity derivative skewness. From measurement, K' was found to be roughly about 0.1.

For an additional justification of Eq. (10), let us first note that $du/dx \sim \varepsilon^{1/2}$ in the dissipation range, so that $d/dx(du/dx) \sim (1/\varepsilon^{1/2})d/dx(\varepsilon)$. In the spirit of the p model [9], we can write $\varepsilon(x) = (\langle \varepsilon \rangle L/\eta)p_1 \cdots p_{k-1}p_k$, and $\varepsilon(x+\eta) = (\langle \varepsilon \rangle L/\eta)p_1 \cdots p_{k-1}(1-p_k)$, where the p_i's assume values of 0.3 or 0.7 with equal probability, and $\eta/L = 2^{-k}$. Therefore,

$$\frac{d}{dx}(\varepsilon) \sim \frac{(1-2p_k)}{p_k}\varepsilon(x) \ , \tag{12}$$

showing that $d/dx(du/dx) \sim (\varepsilon^{1/2}/\eta)$, and $d/dx(d^2u/dx^2) \sim (\varepsilon^{1/2}/\eta^2) \sim 1/\eta^2(du/dx)$, as ascertained before. Notice that the term $(1-2p_k)/p_k$ is of the order unity, and can be positive or negative, just as $K'(x)$ in Eq. (10) above.

Returning now to Eq. (6), we first note that $|\langle \Delta u(r)^n \rangle| = |A_n|[1-n(K/24)(r/\eta)^2]$. Therefore,

$$\log_{10}|\langle \Delta u(r)^n \rangle| = \log_{10}|A_n| + n \log_{10}(r) + \log_{10}\left[1 - \frac{K}{24} n \left[\frac{r}{\eta} \right]^2 \right] \ . \tag{13}$$

Solving for $\log_{10}(r)$ with $n=3$ in Eq. (13) and replacing this expression for $\log_{10}(r)$ back into the equation, we obtain

$$\log_{10}|\langle \Delta u(r)^n \rangle| = \log_{10}|A_n| - \frac{n}{3}\log_{10}|A_3| + \frac{n}{3}\log_{10}|\langle \Delta u(r)^3 \rangle| \ , \tag{14}$$

provided $\log_{10}[1-(K/24)n(r/\eta)^2] \sim -(K/24)n(r/\eta)^2$ is smaller than, say, 0.5. For $K \sim 0.1$ and $n=8$, Eq. (14) can be expected to be valid up to $r \sim 5\eta$.

Equation (14) is identical [10] to Eq. (4), showing that the naive scaling occurs over a larger range than might be expected from first-order Taylor-series expansion. Clearly, if the inertial and dissipative ranges possess the same scaling, the only consistent scenario is for the iner-

tial range exponents to be the Kolmogorov values of $n/3$.

Dissipative range, case A: If the absolute value of odd-order velocity increments is taken before the averaging operation, the averages of various terms in Eq. (5) cannot be obtained as before and $B_{2n+1} \neq 0$. We proceed via Kolmogorov's refined similarity hypotheses [11] according to which

$$\Delta u(r) = V(r\varepsilon_r)^{1/3} , \tag{15}$$

where ε_r is the average of ε over an interval of length r, and V in the inertial range is a universal stochastic variable independent of r and ε_r. We are now interested in Eq. (15) for r in the dissipative range, where, again according to the refined similarity hypothesis, V should depend only on the local Reynolds number $\mathrm{Re}_r = r(r\varepsilon_r)^{1/3}/\nu$. Although we now know that this is not quite correct [8], a good approximation [12] is to assume that V is distributed uniformly on the interval $[-\mathrm{Re}_r/15)^{1/2}, (Re_r/15)^{1/2}]$. It can be shown [13] that the bounds of this interval for V are rigorous. We then find that the expected value of $|\Delta u(r)^n|$ conditioned on $r\varepsilon_r$ is

$$\langle |\Delta u(r)^n| | r\varepsilon_r \rangle \sim r^{n/2}(r\varepsilon_r)^{n/2} . \tag{16}$$

Taking now the expected value with respect to $r\varepsilon_r$, and using the relation [9] that $\langle (r\varepsilon_r)^q \rangle \sim r^{\zeta_{3q}}$, we find that

$$\langle |\Delta u(r)^n| \rangle \sim r^{n/2+\zeta_{3n/2}} . \tag{17}$$

Solving Eq. (17) for r with $n=3$ and replacing r back into it, we find that

$$\langle |\Delta u(r)^n| \rangle \sim \langle |\Delta u(r)^3| \rangle^{\beta_n} , \tag{18}$$

where $\beta_n = (n/2+\zeta_{3n/2})/(3/2+\zeta_{9/2})$. Note that these exponents differ from the corresponding exponents for the case C because we plot $\langle |\Delta u(r)^n| \rangle$ against the third-order moment of the absolute value of the velocity increment.

Inertial range: Returning to Eq. (15), where the stochastic variable V is assumed to be independent of $r\varepsilon_r$, we have

$$\begin{aligned} \langle |\Delta u(r)^n| \rangle &= \langle |V^n| \rangle \langle (r\varepsilon_r)^{1/3} \rangle \sim E_n r^{\zeta_n} , \\ |\langle \Delta u(r)^n \rangle| &= |\langle V^n \rangle| \langle (r\varepsilon_r)^{1/3} \rangle \sim F_n r^{\zeta_n} . \end{aligned} \tag{19}$$

Within the constraints of the refined similarity hypothesis, the scaling exponents are the same for both cases A and C. As we shall see shortly, the two sets of exponents are not the same (although close), thus reflecting that the refined similarity hypothesis is not exact.

Separation of the scaling regimes: To illustrate the two scaling regimes distinguished so far, let us consider the eighth-order moment. The qualitative results are the same for all the other moments. Figure 1 is a plot of $|\langle \Delta u(r)^8 \rangle|$ versus $|\langle \Delta u(r)^3 \rangle|$, where it is shown that the straight-line fits for the dissipative and the inertial ranges yield slopes of 2.66 and 2.05, respectively. It is indeed possible to obtain a compromise fit for a single slope that spans both ranges. The slope then is 2.49. However, it is

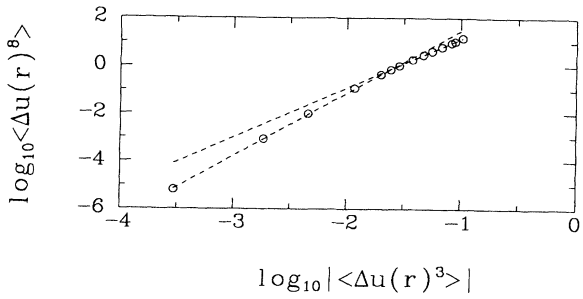

FIG. 1. Plots of $\log_{10}\langle \Delta u^8 \rangle$ vs $\log_{10}|\langle \Delta u^3 \rangle|$. The first seven points (that span the dissipative range) and the following seven points (that span the inertial range) are fitted separately and shown as dashed lines. The smaller slope corresponds to the inertial range is 2.05. The greater slope is 2.66 and corresponds to the dissipative range.

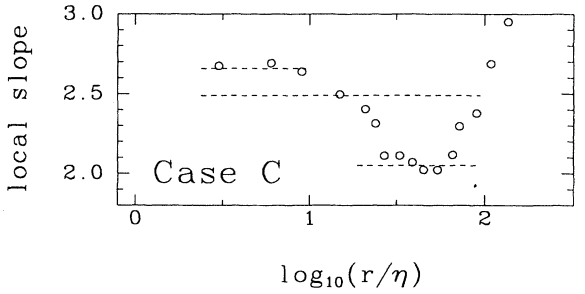

FIG. 2. Local slopes of the plot of Fig. 2, as a function of $\log_{10}(r/\eta)$. The two regions where the local slope is approximately constant correspond to the dissipative and inertial ranges. The dashed lines correspond to slopes of 2.66, 2.49, and 2.05. The intermediate value is the slope of a brute-force straight-line fit to the entire range of data.

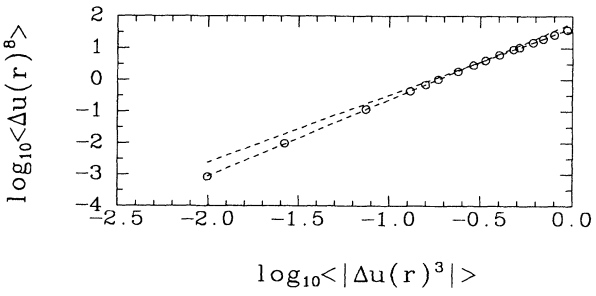

FIG. 3. Plots of $\log_{10}\langle |\Delta u(r)|^8 \rangle$ vs $\log_{10}\langle |\Delta u(r)|^3 \rangle$. The first seven points (that span the dissipative range) and the following seven points (that span the inertial range) are fitted separately and shown as dashed lines. The smaller slope corresponds to the inertial range and is 2.12. The greater slope is 2.42 and corresponds to the dissipative range.

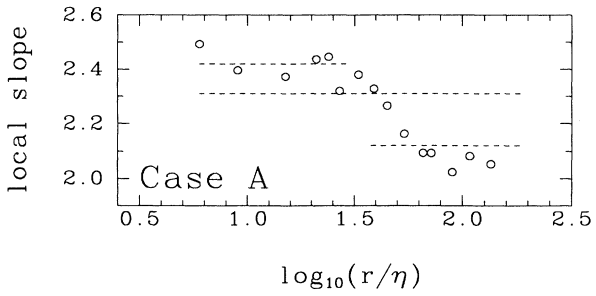

FIG. 4. Local slopes of the plot of Fig. 3, as a function of $\log_{10}(r/\eta)$. The two regions where the local slope is approximately constant correspond to the dissipative and inertial ranges. The dashed lines correspond to slopes of 2.42, 2.31, and 2.12. As in Fig. 2, the intermediate value is the slope of a brute-force straight-line fit to the entire range of data.

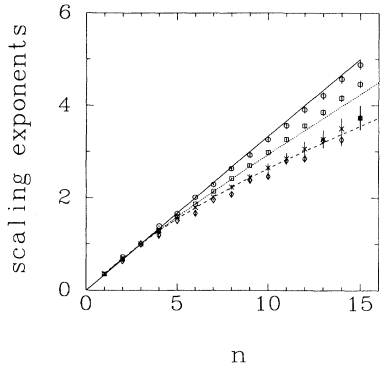

FIG. 5. Scaling exponents ζ_n in $|\langle \Delta u(r)^n \rangle| \sim |\langle \Delta u(r)^3 \rangle|^{\zeta_n}$ for the dissipative range (circles) and the inertial range (diamonds) with their error bars. The solid line is $n/3$ and the dashed line is ζ_n from the p model [9]. The squares and crosses are the scaling exponents in $\langle |\Delta u^n| \rangle \sim \langle |\Delta u^3| \rangle^{\zeta_n^*}$ for the dissipative and inertial ranges, respectively. The dotted line corresponds to the exponents β_n defined after Eq. (18).

misleading to do so, as can be seen in Fig. 2, which shows a plot of the local slope $d \log|\langle \Delta u(r)^8 \rangle| / d \log_{10}|\langle \Delta u(r)^3 \rangle|$ as a function of $\log_{10}(r)$. Two flat regions can be observed, corresponding to the separate scaling regimes of Fig. 1. The compromise slope of Fig. 1 corresponds to the intermediate horizontal line in Fig. 2. Two separate scaling regions indeed appear to be evident.

Figures 3 and 4 are the result of a similar analysis for the case *A*. Again, two scaling regimes can be seen.

Figure 5 shows a summary of the scaling exponents measured. The circles and diamonds correspond, for case *C*, to the dissipative and inertial ranges, respectively. The solid line with slope $n/3$ is the prediction for the slope in the dissipative range. The slight departure observed from this line is within the uncertainty of measurements. Squares and crosses correspond to case *A*. The dotted line corresponds to β_n defined after Eq. (18), and we used the p model [9] to represent the function ζ_n (dashed line). Note, in particular, that the scaling exponents for even- and odd-order structure functions behave differently for case *C*; the odd-order moments fall on a curve that is distinct from that connecting even-order ones.

In conclusion, the present results show that, while the notion of an extended range of scaling is not obtained for high-order moments, it helps highlight the existence of two distinct scaling regions. Different scaling exponents are obtained, depending on whether one considers the classical structure functions or moments of absolute values of velocity increments. In either case, deviations from the Kolmogorov scaling appear real in the inertial range.

We thank Dr. D. P. Lathrop for some helpful discussions and Professor L. Sirovich for bringing Ref. [4] to our attention.

[1] A. S. Monin and A. M. Yaglom, *Statistical Fluid Mechanics* (MIT, Cambridge, MA, 1971), Vol. II.

[2] F. Anselmet, Y. Gagne, E. J. Hopfinger, and R. A. Antonia, J. Fluid. Mech. **140**, 63 (1984).

[3] A. N. Kolmogorov, C. R. Acad. Sci. USSR **30**, 299 (1941).

[4] R. Benzi, S. Ciliberto, R. Tripiccione, C. Baudet, F. Massaioli, and S. Succi, Università di Roma, Report No. ROM 2F/92/54 (unpublished).

[5] A. N. Kolmogorov, Dokl. Akad. Nauk SSSR **32**, 19 (1941).

[6] C. Meneveau and K. R. Sreenivasan, J. Fluid Mech. **224**, 429 (1991). The flow is a turbulent boundary layer in air, developing on a smooth flat plate. The microscale Reynolds number is about 190. Velocity measurements were made with a hot wire located at 0.2δ, where δ is the thickness of the boundary layer.

[7] L. Zubair, Ph.D. thesis, Yale University, 1993.

[8] G. Stolovitzky, P. Kailasnath, and K. R. Sreenivasan, Phys. Rev. Lett. **69**, 1178 (1992).

[9] C. Meneveau and K. R. Sreenivasan, Phys. Rev. Lett. **59**, 1424 (1987).

[10] Equation (14) can also be obtained by expanding $\log_{10}|\langle \Delta u(r)^n \rangle|$ in a Taylor series of $\log_{10}(r)$ in the form $\log_{10}|\langle \Delta u(r)^n \rangle| = E_n + F_n \log_{10}(r) + G_n [\log_{10}(r)]^2$, and noting from experiment that $G_n = QF_n$, where Q is independent of n and r and the ratio F_n/F_3 is equal to $n/3$.

[11] A. N. Kolmogorov, J. Fluid Mech. **13**, 82 (1962).

[12] G. Stolovitzky and K. R. Sreenivasan (unpublished).

[13] As $\Delta u(r) = \int_x^{x+r} (du/dx) dx$, we have from Schwarz inequality that $|\Delta u(r)| \le [\int_x^{x+r} 1^2 dx \int_x^{x+r} (du/dx)^2 dx]^{1/2}$. By definition, $|V| = |\Delta u|/(r\varepsilon_r)^{1/3}$, and $r\varepsilon_r = 15\nu \int_x^{x+r} (du/dx)^2 dx$. We then find $|V| \le r^{1/2} (r\varepsilon_r)^{1/6} / (15\nu) = (\mathrm{Re}_r/15)^{1/2}$.